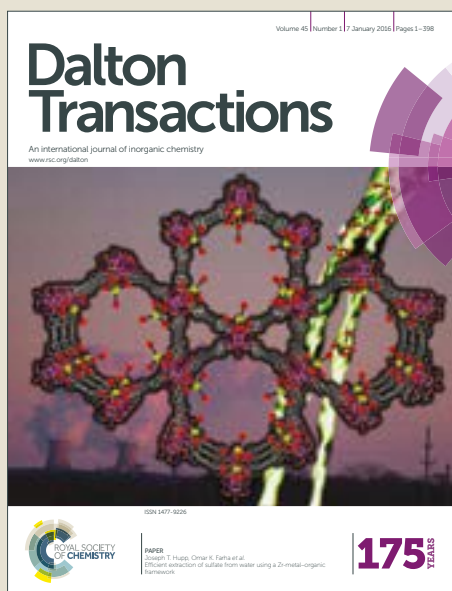


Dalton Transactions

Accepted Manuscript



This article can be cited before page numbers have been issued, to do this please use: Y. Niu, Q. Xu, Y. Wang, Z. Li, J. Lu, P. Ma, C. Zhang, J. Niu and J. Wang, *Dalton Trans.*, 2018, DOI: 10.1039/C8DT01243A.



This is an Accepted Manuscript, which has been through the Royal Society of Chemistry peer review process and has been accepted for publication.

Accepted Manuscripts are published online shortly after acceptance, before technical editing, formatting and proof reading. Using this free service, authors can make their results available to the community, in citable form, before we publish the edited article. We will replace this Accepted Manuscript with the edited and formatted Advance Article as soon as it is available.

You can find more information about Accepted Manuscripts in the [author guidelines](#).

Please note that technical editing may introduce minor changes to the text and/or graphics, which may alter content. The journal's standard [Terms & Conditions](#) and the ethical guidelines, outlined in our [author and reviewer resource centre](#), still apply. In no event shall the Royal Society of Chemistry be held responsible for any errors or omissions in this Accepted Manuscript or any consequences arising from the use of any information it contains.



Journal Name

ARTICLE

Preparation, characterization, and catalytic performances of a pyrazine dicarboxylate-bridging rare-earth-containing polytungstoarsenate aggregate for selective oxidation of thiophenes and deep desulfurization of model fuels

Received 00th January 20xx,
Accepted 00th January 20xx

DOI: 10.1039/x0xx00000x

www.rsc.org/

Yanjun Niu, Qiaofei Xu, Yuan Wang, Zhao Li, Jingkun Lu, Pengtao Ma, Chao Zhang, Jingyang Niu* and Jingping Wang*

A new polytungstoarsenate: $K_6LiH_6[Ce_2(H_2O)_{14}(pzdc)(H_2pzdc)As_3W_{29}O_{103}] \cdot 22H_2O$ (**1**) ($H_2pzdc = 2,3$ -pyrazinedicarboxylic acid) is synthesized through conventional aqueous solution method. In this synthetic approach, organic ligand pyrazine dicarboxylate acid was induced into the arsenotungstates system. The synthesized compound **1** was well characterized by elemental analysis, IR spectroscopy, UV-vis spectroscopy, thermogravimetric analysis (TGA), powder X-ray diffraction (PXRD), and single-crystal X-ray diffraction. The catalytic activity of compound **1** was tested in acetonitrile to oxidize organosulfur compounds (benzothiophene (BT) and dibenzothiophene (DBT)) by hydrogen peroxide as an oxidant, at room temperature. Two substrates were oxidized to their corresponding sulfones with high conversion and selectivity. Taking advantage of this remarkable catalytic move, the $1/H_2O_2/CH_3CN$ system was further utilized in the oxidation of model fuels (MF) including a mixture of BT and DBT in octane. As a result, the organosulfur compounds in the model fuels were fully converted into their corresponding sulfones. What's more, the fluorescence properties of **1** have also been investigated.

Introduction

Design and synthesis of polyoxometalate (POM)-based polymers are of great significance in broad area of research. Polyoxometalates (POMs), as a large family of well-defined inorganic metal-oxygen cluster anions with abundant topologies and high negative charge, have been widely employed in several fields,¹ one of the most important being the acid and oxidative catalysis.² More importantly, the POM-based complexes can join with lanthanide (Ln) ions, transitional metal (TM) ions, and/or heterometallic clusters, bringing in various functionalities and significant applications in catalysis, sensing, imaging, medicine, and multifunctional materials.³ As we know, an increasing amount attention has been directed on POMs Lanthanum chemistry, as oxophilic nature of Ln ions primarily more responsible for the formation of POM-based Ln complexes. Ln ions can easily react with oxygen-rich POMs, usually resulting in over-quick precipitation while not crystalline products.⁴ Thus, to isolate the single

crystals of such compounds are rather difficult compared with the TM-containing POMs.⁴ Up to now, varieties of Ln-based phosphotungstates, silicotungstates, and germanotungstates have been widely reported since 1971.⁵ However, exploration of Ln-arsenotungstates are still relatively rare in spite of the high nucleophilicity of that arsenotungstates based polyanions.⁶ Moreover, it is important to say that, organic ligands may play an important role in the molecular designing of elaborate Ln-containing POMs. On one hand, they could interact with rare earth ions first, which can effectively prevent rare earth ions from precipitating by reducing the reactivity of rare earth ions with POMs. On the other hand, the organic ligands may stabilize the polyoxoanions by various non-covalent interactions. Currently, the majority of Ln-containing arsenotungstates are mainly monocarboxylic-based or purely inorganic ones, such as $[As_{12}Ce_{16}(H_2O)_{36}W_{148}O_{524}]^{76-}$,⁷ $[Ln_{16}As_{16}W_{164}O_{576}(OH)_8(H_2O)_{42}]^{80-}$,⁸ $[(H_2O)_{10}Ln^{III}(Ln^{III}_2OH)(B-\alpha-AsW_9O_{33})_4(WO_2)_4]^{40-}$,⁹ $[Gd_8As_{12}W_{124}O_{432}(H_2O)_{22}]^{60-}$,¹⁰ $[Gd_6As_6W_{65}O_{229}(OH)_4(H_2O)_{12}(OAc)_2]^{38-}$,¹⁰ $[Yb_{10}As_{10}W_{88}O_{308}(OH)_8(H_2O)_{28}(OAc)_4]^{40-}$,¹¹ $[Ce_4As_4W_{44}O_{151}(alanine)_4(OH)_2(H_2O)_{10}]^{12-}$,¹² $[Ln_4As_5W_{40}O_{144}(H_2O)_{10}(Gly)_2]^{21-}$,¹³ $[Tb_2(pic)(H_2O)_2(B-B-AsW_8O_{30})_2(WO_2(pic))_3]^{10-}$,¹⁴ and $[Tb_8(pic)_6(H_2O)_{22}(B-B-AsW_8O_{30})_4(WO_2(pic))_6]^{12-}$.¹⁴ Ln-containing arsenotungstates with multicarboxylic ligands are not so usual in the past reports. Hence, it is significant and challenging to synthesize new compounds starting from the $[As_2W_{19}O_{67}(H_2O)]^{14-}$ with polycarboxylic acid ligand. Recently, Our group have obtained

^a Henan Key Laboratory of Polyoxometalate Chemistry, Institute of Molecular and Crystal Engineering, College of Chemistry and Chemical Engineering, Henan University, Kaifeng 475004, Henan, China. E-mail: jyniu@henu.edu.cn, jpwang@henu.edu.cn; Fax: (+86)371-23886876

[†] Electronic supplementary information (ESI) available: structural figure (Fig S1); IR spectra, XPRD and TGA of **1** (Fig S2–S4); the UV-vis spectra of **1** with 5×10^{-5} mol/L in aqueous solution (Figure S5); the UV-vis spectra of **1** at different pH values (Figure S6); Catalytic properties. CCDC reference numbers 1817478 for **1**. See DOI: 10.1039/x0xx00000x.

a series of giant organic–inorganic Ln-containing POM–carboxylate clusters on $[\text{As}_2\text{W}_{19}\text{O}_{67}(\text{H}_2\text{O})]^{14-}$ including $\text{K}_{14}\text{Li}_4\text{H}_{20}[\text{As}_6\text{W}_{58}\text{O}_{206}\text{Ce}_4(\text{pydc})_2(\text{H}_2\text{O})_6]\cdot 44\text{H}_2\text{O}$ (H_2pydc = pyridine-2,3-dicarboxylic acid),¹⁵ $\text{K}_{13}\text{LiH}_4[\text{RE}_2(\text{C}_4\text{H}_4\text{O}_6)(\text{C}_4\text{H}_2\text{O}_6)(\text{AsW}_9\text{O}_{33})]_2\cdot 28\text{H}_2\text{O}$ ¹⁶ (RE = Ho, Er), $\text{K}_9\text{LiH}_8[\text{RE}_2(\text{C}_4\text{H}_4\text{O}_6)(\text{C}_4\text{H}_2\text{O}_6)(\text{AsW}_9\text{O}_{33})]_2\cdot n\text{H}_2\text{O}$ (RE = Tm, Yb, Lu, Y),¹⁶ and $\text{K}_{11}\text{LiH}_{21}[\text{RE}_3(\text{H}_2\text{O})_7\{\text{RE}_2(\text{H}_2\text{O})_4\text{As}_2\text{W}_{19}\text{O}_{68}(\text{WO}_2)_2(\text{C}_6\text{O}_7\text{H}_4)_2\}_3]\cdot n\text{H}_2\text{O}$ (RE = Y, Tb, Dy, Ho, Er, Tm, Yb, Lu).¹⁷

Organic ligands like 2,3-pyrazine dicarboxylic (H_2pzdc) acid, is a remarkable multidentate ligand with two oxygen and two nitrogen donors,¹⁸ which is a diverse class of oxidation catalyst, which can also be efficiently used as co-catalyst in numerous catalytic reactions or as ligand to synthesize novel POMs or metal complex catalytic systems.¹⁹ Furthermore, the dilacunar species $[\text{As}_2\text{W}_{19}\text{O}_{67}(\text{H}_2\text{O})]^{14-}$, which possess the ability to dissociate and rearrange, could accelerate the generation of a numerous of POM-based building blocks in solution.¹⁷ Therefore, $[\text{As}_2\text{W}_{19}\text{O}_{67}(\text{H}_2\text{O})]^{14-}$, the preformed precursor could be regarded as an applicable candidate for the step-by-step assembly of charming cluster architectures. Till now, the application of arsenotungstates has been poorly explored for the catalytic oxidation, most likely because of the toxicity of arsenic.²⁰ However, for academic reasons, the catalytic ability of arsenotungstates would be imperative and attractive. Nowadays, the interest in developing efficient catalytic systems of POMs for the oxidation of organosulfur compounds is of great relevance in the context of the preparation of synthetically useful sulfoxides and sulfones, as well as of the desulfurization of fuels.²¹ Moreover, the oxidative desulfurization (ODS) of fuels constitutes a high potential process in terms of efficiency and environmental sustainability.²² More than 80% of the total sulfur content in diesel fuel are thiophene sulfides, and benzothiophene (BT) and dibenzothiophene (DBT) account for 70% of thiophene sulfides. Thus, removal of thiophene sulfides is of great importance in industry.²³ To date, numerous reports have shown that the excellent catalytic properties of POMs qualifies them as prime candidates for the ODS.

Herein, the dilacunar POM $[\text{As}_2\text{W}_{19}\text{O}_{67}(\text{H}_2\text{O})]^{14-}$ was utilized as basic building block, and 2,3-pyrazinedicarboxylic acid (H_2pzdc) and rare earth cations as the bridging fragments were induced to the system with the purpose of isolating new POM based compounds via the building block approach. As expected, we successfully synthesized a new polytungstoarsenate:

$\text{K}_6\text{LiH}_6[\text{Ce}_4(\text{H}_2\text{O})_{14}(\text{pzdc})(\text{H}_2\text{pzdc})\text{As}_3\text{W}_{29}\text{O}_{103}]\cdot 22\text{H}_2\text{O}$ (**1**) and employed this compound for selective oxidation of thiophenes and deep desulfurization of model fuels. This compound as a heterogeneous catalyst shows efficiently catalytic activity in the oxidation system under mild conditions.

Experimental

Materials and methods

$\text{K}_{14}[\text{As}_2\text{W}_{19}\text{O}_{67}(\text{H}_2\text{O})]$ was prepared according to the literature²⁴ and confirmed by IR spectrum. All other chemical reagents were purchased and used without further purification. Elemental analysis (C, H, N) was conducted on a PerkinElmer 2400-II CHNS/O analyzer. ICP analysis was performed on a PerkinElmer Optima 2000 ICP-OES spectrometer. IR spectrum was obtained from a solid sample pelletized with KBr pellets on a Bruker VERTEX 70 in the range of 4000–400 cm^{-1} . Thermogravimetric (TG) analysis was carried out on a Mettler-Toledo TGA/SDTA 851^e thermal analyzer in a flowing nitrogen air atmosphere in the temperature region of 25–800 °C with a heating rate of 10 °C·min⁻¹. UV spectrum was obtained on a U–4100 spectrometer at room temperature in the range of 400–200 nm (distilled water as solvent). PXRD was performed on Bruker AXS D8 Advance diffractometer instrument with Cu K α radiation ($\lambda = 1.54056 \text{ \AA}$) in the range $2\theta = 5\text{--}45^\circ$ at 296 K. Photoluminescence properties were performed on F-7000 fluorescence spectrophotometer. The oxidation products were identified and quantitatively analyzed by Agilent Technologies 7890B/5977B GC-MS instrument and BRUKER 450-GC instrument with a flame-ionization detector (FID).

Synthesis of compound 1

A sample of 2,3-pyrazinedicarboxylic acid (0.063g, 0.375 mmol) and $\text{CeCl}_3\cdot 7\text{H}_2\text{O}$ (0.1118g, 0.30 mmol) was dissolved in 15 mL distilled water, then $\text{K}_{14}[\text{As}_2\text{W}_{19}\text{O}_{67}(\text{H}_2\text{O})]$ (0.658g, 0.125 mmol) and lithium chloride (0.1 g) were added under stirring at room temperature. Ten minutes later, the pH of the solution was carefully adjusted to about 4.5 with 1 mol·L⁻¹ lithium hydroxide and then the mixture were heated to 60 °C for 1 h. After cooling to room temperature, the clear solution was allowed to stand for crystallization. Yellow hexagonal crystals were collected 2-3 weeks later. Yield: 0.47 g (65.38% based on Ce). Elemental analysis (%) calcd for **1**: C, 1.60; H, 0.94; N, 0.62; K, 2.61; Li: 0.078, Ce, 6.23; As, 2.50; W, 59.27. Found for **1**: C, 1.51; H, 1.01; N, 0.62; K, 2.72; Li: 0.082, Ce, 6.34; As, 2.63; W, 59.12. Selected IR (KBr, cm^{-1}): 3429 (br), 1623 (s), 1451 (m), 1395 (m), 1364 (w), 1236 (w), 1206 (w), 1170 (w), 1120 (m), 943 (s), 861 (s), 790 (s), 717 (s), 650 (w), 499 (w).

X-ray crystallography

Suitable single crystal of **1** was prudentially selected and encapsulated in a capillary tube. Intensity data was collected on a Bruker APEX-II detector at 296(2) K using graphite-monochromated Mo K α radiation ($\lambda = 0.71073 \text{ \AA}$). Routine Lorentz and polarization corrections were applied, and a multi-scan absorption correction was performed using the SADABS program. The structure was solved by direct methods, and refinement was done by full-matrix least-squares against F^2 on all data using the SHELXTL program suite.²⁵ In the final refinement, the W, As, Ce, and K atoms were refined anisotropically; the O, C and N atoms were refined isotropically. All hydrogen atoms were refined isotropically as a riding mode using the default SHELXTL parameters. A summary of crystal data and structure refinement parameters are listed in Table 1 and CCDC 1817478 contains the supplementary crystallographic data for this paper.

Table 1 The data collection and refinement parameters of compound **1**

Formula	C ₁₂ H ₄ As ₃ Ce ₄ K ₆ N ₄ O ₁₄₇ W ₂₉
Mr(g.mol ⁻¹)	8907.68
T (K)	296.15
Crystal system	Triclinic
space group	<i>P</i> -1
a (Å)	19.533(2)
b (Å)	20.652(2)
c (Å)	25.774(3)
α (deg)	96.152(2)
β (deg)	104.376(2)
γ (deg)	116.764(2)
V (Å ³)	8699.8(17)
Z	2
Dc(g. cm ⁻³)	3.400
μ (mm ⁻¹)	20.914
limiting indices	-21 ≤ h ≤ 23, -20 ≤ k ≤ 24, -30 ≤ l ≤ 27
Params	1040
reflins collected	44392
GOF	1.001
R ₁ , wR ₂ [I > 2σ (I)]	0.0709, 0.1686
R ₁ , wR ₂ [all data]	0.1361, 0.2079

Typical procedure for the oxidation reactions

The catalytic oxidation reactions were studied as follows: the substrate (0.6 mmol), the catalyst (the ratio of substrate/catalyst (S/C) = 300, 500, 800, 1000, 1200 or 1500), H₂O₂ (0.6 mmol, H₂O₂/substrate (O/S) = 1; 1.2 mmol, H₂O₂/substrate (O/S) = 2; 1.8 mmol, H₂O₂/substrate (O/S) = 3), 2.0 mL of acetonitrile and the internal standard (toluene, 0.6 mmol) were stirred in a 50ml round-bottom tube at room temperature (25 °C). To monitor the oxidation reactions, small aliquots from the reaction mixture were directly injected into a GC-FID apparatus at regular intervals.

The experiments of the oxidation of model fuels (MFs) were carried out as follows: two substrates (0.06 mmol of DBT and BT, respectively, a total of 0.12 mmol) and the catalyst were dissolved in 500 μL of CH₃CN, and the total reaction volume was completed with 1.5 mL of octane. Addition of H₂O₂ and completion of the reaction were done as indicated above.

Instruments and methods

GC-FID and GC-MS analyses were performed as previously described.²⁶ Values of the conversion and selectivity were estimated from the corresponding chromatographic peak areas using toluene as the internal standard. To confirm the structure of the obtained products, the retention times in the GC-FID were compared with those of authentic samples identified previously, and the reaction mixtures were also injected into the GC-MS.²⁶

Results and discussion

Structural descriptions

Bond valence sum calculations^{12, 15, 27} indicate that the oxidation states of all W, As, and Ce centers exhibit +6, +3, and +3, respectively. Single-crystal X-ray diffraction analysis indicates that **1** consists of the polyoxoanion [Ce₄(H₂O)₁₄(pzdc)(H₂pzdc)As₃W₂₉O₁₀₃]¹³⁻ (abbreviated to {Ce₄As₃W₂₉}), 22 lattice water molecules, 6 K⁺ counterions, 6 protons based on charge balance and one Li⁺ ion on the basis of elemental analysis. The polyanion {Ce₄As₃W₂₉} in **1** is constructed from four Ce³⁺, a pzdc ligand, a H₂pzdc ligand and a {As₃W₂₉} building block, which is analogous to the subunit [As₃W₂₉O₁₀₃Ce₂(pydc)(H₂O)₃]¹⁹⁻ of the polyanion [As₆W₅₈O₂₀₆Ce₄(pydc)₂(H₂O)₆]³⁸⁻ reported by our group previously.¹⁵ The {As₃W₂₉} building block in **1** contains three identical {α-AsW₉O₃₃} units, which are linked to each other via two tungsten atoms (W(10) and W(20)) and a cerium atoms (Ce(1)) (Fig. 1a). It is prominent that four cerium cations in **1** exhibit distinct geometry configurations. Ce(1)³⁺ (Fig. 2a) is nine-coordinate and adopts, distorted monocapped square antiprismatic geometry, which is defined by six terminal oxygen atoms from a {As₃W₂₉} cluster [Ce(1)–O: 2.504(19)–2.588(19) Å], a carboxyl oxygen atom [Ce(1)–O: 2.576(18) Å] and a nitrogen atom [Ce(1)–N: 2.66(2) Å] from a pzdc ligand, and a terminal water ligand [Ce(1)–O: 2.503(18) Å]. Ce(1)³⁺ is embed in {As₃W₂₉} and bridged with two additional tungsten atoms forming a closed triangular structure, and further stabilize the crystal structure. Differently, Ce(3)³⁺ (Fig. 2c), inlaid in {As₃W₂₉} as Ce(1)³⁺, is ten-coordinate and adopts a bicapped square antiprismatic geometry, which bonds to four terminal oxygen atoms from a {As₃W₂₉} cluster [Ce(3)–O: 2.423(18)–2.531(17) Å], four carboxyl oxygen atoms [Ce(3)–O: 2.67(2)–2.75(2) Å] from the ligands, and two terminal water ligands [Ce(3)–O: 2.64(2)–2.64(2) Å]. By the bonding effect of Ce(3)³⁺ (Ce3–O108–C11 and Ce3–O109–C11), the two polyanions are giving rise to a dimer (Fig. 1b). The dimer is arranged in a crossed form, obviously, which is much lower than the overlapping type in the view of the energy, and more beneficial to improve the stability of the compound. Ce(2)³⁺ (Fig. 2b) is nine-coordinate, in a monocapped square antiprismatic geometry as Ce(1)³⁺, which is defined by one terminal oxygen atoms from a {As₃W₂₉} cluster [Ce(2)–O: 2.534(19) Å], a carboxyl oxygen atom [Ce(2)–O: 2.41(3) Å] and a nitrogen atom [Ce(1)–N: 2.67(3) Å] from a pzdc ligand, and five terminal water ligand [Ce(2)–O: 2.58(3)–2.68(3) Å]. One of the carboxyl oxygen atoms O104 is coordinated with Ce2 of the adjacent dimer, leading to a novel 1-D chain structure. Ce(4)³⁺ (Fig. 2d) is nine-coordinate and monocapped square antiprismatic geometry, which bonds to three terminal oxygen atoms from a {As₃W₂₉} cluster [Ce(4)–O: 2.472(18)–2.49(2) Å], and six terminal water ligands [Ce(4)–O: 2.52(3)–2.62(3) Å]. The bonding effect of Ce(4)³⁺ with the terminal oxygen atom O11 (O67–Ce4–O11, O102–Ce4–O11) from a {As₃W₂₉} cluster and the adjacent dimer, leading to a 2-D planar structure (Figure 1c). Moreover, the polyoxoanion are connected by K⁺ resulting in the 3D framework (Figure S1 in the ESI[†]).

FT-IR and XRPD patterns

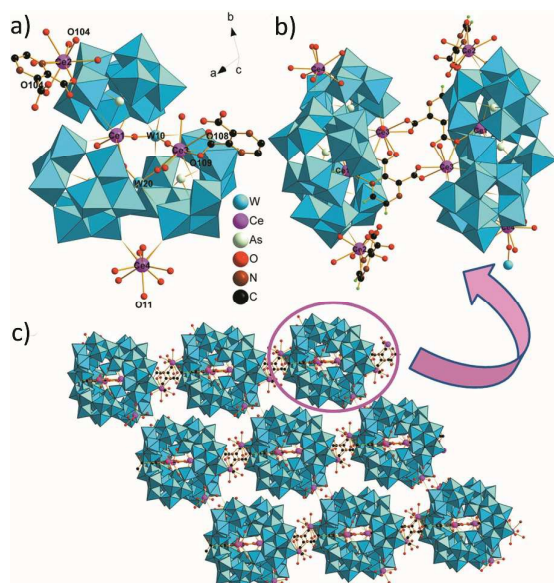


Fig. 1 a) Polyhedral and ball-and-stick representation of the macroanion $[\text{As}_3\text{W}_{29}\text{O}_{103}\text{Ce}_4(\text{pzdc})_2(\text{H}_2\text{pzdc})_2(\text{H}_2\text{O})_{14}]^{13-}$ in **1**; b) the dimer of **1**; c) View of the 2D framework of **1**.

The IR spectrum of **1** (Fig S2 in the ESI[†]) shows a broad peak at 3429 cm^{-1} and a strong peak at 1623 cm^{-1} attributed to the lattice and coordinated water molecules. The characteristic vibration patterns for the polyoxoanion frameworks in the low-wavenumber region $500\text{--}1000\text{ cm}^{-1}$ are observed. The peak at 943 cm^{-1} can be attributed to the $\text{W}=\text{O}$ stretching vibration, peaks at 861 and 790 cm^{-1} correspond to the two types of $\text{W}-\text{O}-\text{W}$ stretching vibrations, and the peak at 717 cm^{-1} can be assigned to the $\text{W}-\text{O}(\text{As})$ stretch.¹² Additionally, the stretching vibration of $\text{C}-\text{O}$ (Ln) can be responsible for the peaks at 1120 cm^{-1} and 1071 cm^{-1} .^{12,13} The peaks at 1395 cm^{-1} and 1451 cm^{-1} are assigned to the symmetric stretching vibration of the carboxylate groups,^{12,13} which shift to some extent compared with the free H_2pzdc ligand, indicating that the free H_2pzdc ligand coordinates to the Ce^{3+} cation.

The powder X-ray diffraction pattern of **1** is in good agreement with the simulated pattern based on the single-crystal solution (Fig S3 in the ESI[†]), indicating the phase purity of the product. The differences in intensity may be due to the preferred orientation of the powder samples.

UV spectra

The UV spectrum of compound **1** ($5 \times 10^{-5}\text{ mol L}^{-1}$) in aqueous solution displays an absorption band at $250\text{--}254\text{ nm}$ (Fig S5 and Fig S6 in the ESI[†]). The energy band can be assigned to the $\pi-\pi^*$ charge-transfer transitions of the $\text{O}_{b,c} \rightarrow \text{W}$ bands, indicating the formation of polyoxoanions.²⁸ In order to investigate the stability of the solution of **1**, the in situ spectroscopic measurements were performed in the aqueous system. Both the position and the strength of the absorption bands of compounds **1** do not change, indicating that compounds **1** may be stable in the aqueous system at ambient temperature for 5 hours.

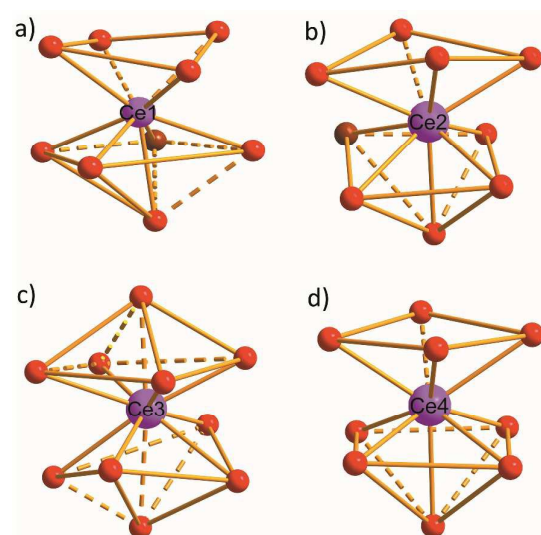


Fig. 2 a) Distorted monocapped square antiprismatic geometry of $\text{Ce}(1)^{3+}$ in **1**; b) monocapped square antiprismatic geometry of $\text{Ce}(2)^{3+}$ in **1**; c) bicapped square antiprismatic geometry of $\text{Ce}(3)^{3+}$ in **1**; d) monocapped square antiprismatic geometry of $\text{Ce}(4)^{3+}$ in **1**.

It is well known that the POMs are commonly sensitive to the pH value of the studied media. Therefore, in order to investigate the influence of the pH values on the stability of compounds in aqueous solution, **1** has been elaborately probed by means of UV-vis spectra. Diluted HCl solution and LiOH solution were used to adjust the pH values in the acidic direction and in the alkaline direction, respectively. The initial pH value of **1** in water was 5.05. As indicated in Fig S6 in the ESI[†], the UV spectrum of **1** in aqueous solution displays an absorption band at $250\text{--}254\text{ nm}$, and the UV spectrum of **1** does not change at all even when the pH value has been lowered to 1.12. In contrast, when increasing the pH value of **1**, the absorbance band at 252 nm is gradually blue-shifted and becomes weaker and weaker, suggesting the decomposition of the POM skeleton of **1**.²⁸ This phenomenon is especially obvious when the pH is higher than 11.05, which indicates that the POM skeleton of **1** is distinctly destroyed at pH higher than 11.05. The results above reveal that compound **1** could exist in a solution whose pH is 1.12–5.05.

Photoluminescence

The solid-state photoluminescent properties of **1** (Figure S4 in the ESI[†]) were measured at room temperature. In order to understand the nature of the emission bands, the photoluminescent properties of free H_2pzdc were also studied. When **1** and free H_2pzdc was excited at 400 nm , they all exhibited a low intensity emission peaks at 601 nm and a high intensity emission peak at 624 nm , which indicated the intraligand energy-transfer process due to the $\pi-\pi^*$ or $n-\pi^*$ transitions.²⁹ However, the success of the transfer of energy to the lanthanide ion from H_2pzdc results in a weaker emission compared **1** with the ligand.²⁹ Thus, the emission bands of **1** may be assigned to the interaction among $\pi-\pi^*$, $n-\pi^*$ and LMCT of H_2pzdc .²⁹

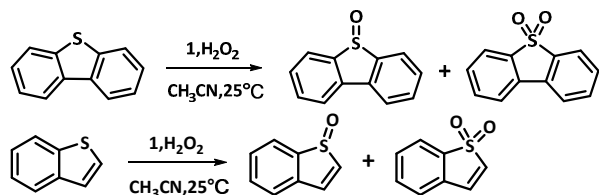
Oxidation of the organosulfur compounds in acetonitrile

We first employed **1** as the catalyst to investigate the oxidation of DBT by using 30% H₂O₂ as oxidant at room temperature in different solvents (Table 2). The results show that the reaction is sensitive to solvent. Polar solvents are suitable for the oxidation reaction. Low conversion was obtained in the nonpolar solvent, such as octane (entry 2) since the solubility of the catalyst in that solvent. CH₃CN is the best solvent to provide the highest conversion (100%). As mentioned above, only the corresponding sulfones are observed at the end of the reactions in most cases. Sulfoxides could only be detected by just switching the solvent to CH₃CH₂OH. The reaction almost did not occur at 25 °C with TBHP or O₂ as an oxidant (entry 7-9). Except for its catalytic oxidation activities, H₂O₂ is better than TBHP as an oxidant on the basis of the environmentally benign property.

Oxidation of DBT under different temperatures with the change of reaction time was investigated as well. The reaction system reaches 100% conversion and 100% selectivity for sulfone after 60, 40, and 30 min, at 40, 35, and 25 °C, respectively. As clearly indicated in Figure 3, a higher reaction temperature can lead to an acceleration of DBT oxidation. On account of the reaction at room temperature (25 °C) for saving energy, room temperature (25 °C) was finally elected for following work in view of the environmentally benign aspect. Typical GC-FID chromatograms illustrating the DBT oxidation reaction profile with H₂O₂ in the presence of **1** for the S/C molar ratio of 300 at different times were shown in Fig. S8.

Fig. 4 illustrates the effect of O/S ratio on the oxidation of DBT. Theoretically, an O/S ratio of 2 is enough for the conversion of DBT into DBTO₂ by stoichiometry. However, a lower conversion of 73.2% at 60 min is observed with an O/S ratio of 2, probably by reason of the decomposition of H₂O₂.³⁰ With an increase in O/S ratio from 2 to 3, the conversion at 60 min increases significantly from 73.2% to 100%. Considering the limited improvement with a further increase to 4, O/S = 3 is chosen as the optimal value for the most recalcitrant substrate. This slight excess is not unusual in the oxidation of this kind of substrate by hydrogen peroxide and catalyzed by POMs, since the O/S molar ratios of 6 : 1,³¹ 8 : 1,³¹ 10 : 1,³² and even to 50 : 1,³³ can be found in the very recent literature.

Due to **1** showed excellent catalytic activity and efficiency in the oxidation of DBT, the oxidation of two model sulfur compounds DBT and BT with different S/C molar ratios has been investigated first. As illustrated in Table 3, it is possible to conclude that good to excellent conversions, ranging from 90 to 100%, were attained with the two substrates for all S/C



Scheme 1. Oxidation of dibenzothiophene (DBT) and benzothiophene (BT) to corresponding sulfoxides and sulfones

Table 2 Oxidation of DBT in Different Solvents^a

Entry	Substrate	Solvent	%Conversion ^d	%Sulfone selectivity
1		/	34	100
2		n-octane	trace	trace
3		CH ₂ Cl ₂	0.2	100
4		CH ₃ CH ₂ OH	56	71
5		CH ₃ CN	100	100
6		H ₂ O	trace	trace
7 ^b		CH ₃ CN	trace	trace
8 ^b		CH ₂ Cl ₂	trace	trace
9 ^c		CH ₃ CN	trace	trace

^a Reaction conditions: the substrate (0.6 mmol), the catalyst corresponding to the substrate/catalyst (S/C) molar ratio of 300; the internal standard (toluene, 0.6 mmol) and H₂O₂ (1.8 mmol) were stirred in 2.0 mL of CH₃CN at room temperature for 1h. ^b TBHP as an oxidant (1.8 mmol). ^c O₂ as an oxidant (1 MPa). ^d Conversion values determined by GC-FID.

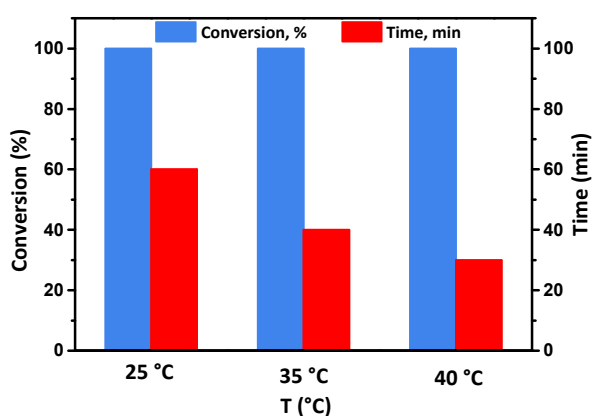


Figure 3 Effect of time and temperature on the oxidation of DBT. Reaction condition: the substrate (0.6 mmol), the catalyst corresponding to the substrate/catalyst (S/C) molar ratio of 300; the internal standard (toluene, 0.6 mmol) and H₂O₂ (1.8 mmol) were stirred in 2.0 mL of CH₃CN.

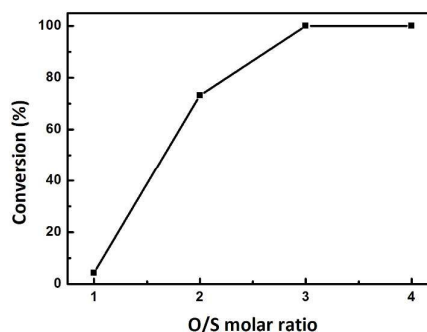


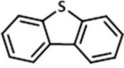
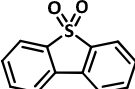
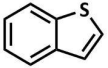
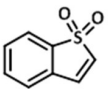
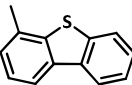
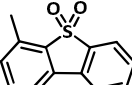
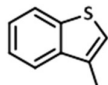
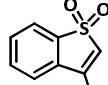
Figure 4 Effect of different O/S ratios on the oxidation of DBT. Reaction condition: the substrate (0.6 mmol), the catalyst corresponding to the substrate/catalyst (S/C) molar ratio of 300; and the internal standard (toluene, 0.6 mmol) were stirred in 2.0 mL of CH₃CN at room temperature for 1h.

molar ratios tested (300, 500, 800, 1000, 1200, 1500). When the ratio of S/C increased, the reaction time increased accordingly, but the oxidation reaction still was steadily accomplished in a short time. Even the ratio reached 1500:1, the reaction smoothly proceeded. As expected, the use of a

ARTICLE

Journal Name

Table 3 Results obtained for the oxidation of DBT, BT, 4-MDBT and 3-MBT with H₂O₂ catalyzed by **1**^a

Substrate	S/C molar ratio	Conversion ^b (%)	Product	Time (min)
	300	100		60
	500	98.5		60
	800	98.1		80
	1000	100		120
	1200	99.1		120
	1500	89.2		120
	300	100		120
	500	99.5		120
	800	96.6		120
	1000	92		150
	1200	96.4		180
	1500	91.2		180
	300	100		60
	500	100		90
	800	100		90
	1000	100		130
	1200	100		150
	1500	100		150
	300	100		90
	500	100		120
	800	100		120
	1000	100		130
	1200	100		150
	1500	96		150

^a Reaction conditions: the substrate (0.6 mmol), the catalyst corresponding to the substrate/catalyst (S/C) molar ratios of 300, 500, 800, 1000, 1200, 1500; the internal standard (toluene, 0.6 mmol) and H₂O₂ (1.8 mmol) were stirred in 2.0 mL of CH₃CN at room temperature. ^b Conversion values determined by GC-FID.

higher amount of the **1** catalyst (S/C molar ratio = 300) affords the best results for each substrate. In particular, the complete oxidation of DBT was attained after 60 min for S/C = 300. As illustrated Table 3, the oxidation reactivities follow the order of DBT > BT. Generally, both electron density and steric hindrance around the sulfur atom have an influence on the reaction activity.³⁴ The electron densities on the sulfur atoms are reported to be 5.739, and 5.758 for BT, and DBT, respectively.³⁴ The lower electron densities on the sulfur of BT lead to its lower reactivities.³⁴ Then the oxidation of two other thiophenic compounds 3-MBT (3-methylbenzothiophene) and 4-MDBT (4-methyldibenzothiophene) has also been investigated under the same experimental conditions (Table 3). The experimental data demonstrate that **1** shows fairly good catalytic activity at room temperature for the sulfur containing substrates. Generally, the use of these POMs as catalysts in sulfoxidation processes requires temperatures around 50–80 °C or even higher. Several previously-reported catalysts on the oxidation of DBT are summarized in Table S1 in the ESI† as the comparative data. The oxidation of various sulphides have studied in the homogeneous situation at room temperature

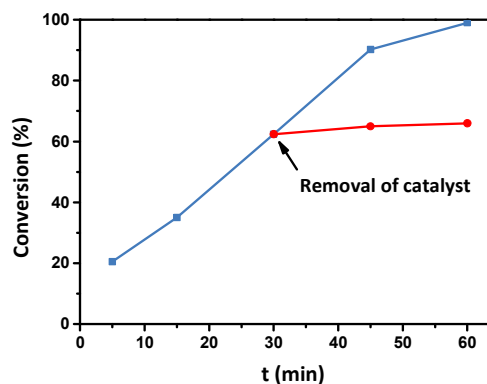


Figure 5 Reaction condition: the substrate (0.6 mmol), the catalyst corresponding to the substrate/catalyst (S/C) molar ratio of 300; the internal standard (toluene, 0.6 mmol) and H₂O₂ (1.8 mmol) were stirred in 2.0 mL of CH₃CN at room temperature.

with H₂O₂ by the group of Mizuno, but the results about the oxidation of DBT was only obtained at 50 °C.³⁵ Obviously, it must be emphasized that **1** is an efficiently catalyst used at room temperature in the sulfoxidation process of recalcitrant thiophenic compounds.

Blank reaction was investigated for DBT, confirming that lower oxidation occurred in the absence of the catalyst (34% conversion for DBT). The parent POM {As₂W₁₉}, H₂pzdc and CeCl₃·7H₂O were used as the catalysts for comparison. The catalytic performances were listed in Table S2 in the ESI†. The conversion of the reaction was 20.4%, 21%, 33% and 100% by using {As₂W₁₉}, CeCl₃·7H₂O, H₂pzdc and compound **1** as catalysts, respectively. Compound **1** displays higher catalytic activity than its parent POM or cerium chloride precursor for the oxidation of DBT to DBTO₂. Meanwhile, a simple mixture of As₂W₁₉, H₂pzdc and CeCl₃·7H₂O had been utilized for the oxidation and showed lower conversion compared with **1** (Table S2 in the ESI†). Therefore, it is suggested that the incorporation of the organic ligand and Ln ion into POM skeleton can enhance the oxidation catalytic activity of the POMs.

To verify whether the observed catalysis is truly heterogeneous or not, the catalytic oxidation of DBT was carried out with **1** under the conditions in Figure 5. After 30min (at 62.4% conversion), the solid **1** was removed from the reaction mixture by filtration and the reaction was allowed to proceed with the filtrate under the same conditions. The results demonstrate the oxidation was completely stopped by removal of **1**. Next, the catalyst was separated by filtration after completion of the oxidation.

The recycling experiments for the oxidation of DBT by 30% H₂O₂ in CH₃CN at room temperature conducted with **1** are shown in Fig S9 in the ESI†. At the end of the reaction, the sample was filtered, washed with CH₃CN, dried at room temperature, and subjected to another cycle. Unfortunately, the recyclability of **1** is not excellent. After three cycles, the desulfurization rate of the catalyst decreases from 100% to 78.3%. This demonstrates that the structure of **1** may be not retaining its skeleton integrity. After three cycles, the ligand fall from the skeleton of POMs, which was deduced by a

comparison of the IR spectra of the used and the fresh catalyst (Fig S10 in the ESI[†]), indicating that the catalyst was not relatively stable in this system.

In the studied oxidation processes, the mechanism may be similar to the one already reported.³⁶ Firstly, the generation of active species occurred by the interaction of the oxidant H₂O₂ with the terminal bonds W^{VI}=O that generates POM peroxo species that can oxidize the sulfur compounds into sulfones. Subsequently, the peroxo species transfer an oxygen atom to the sulfur substrate and the initial W^{VI}=O is regenerated and utilizable again to restart the catalytic cycle.

Oxidation of the organosulfur compounds in model oil

Based on the promising results achieved for the recalcitrant organosulfur compounds described above, the catalytic performance of **1** was evaluated for the oxidation of model fuel (MF), consisting of a mixture of DBT and BT, in octane. The reactions occurred in a CH₃CN/octane (1:3) medium at room temperature.³⁶ The solvent mixtures are very common in this type of study, as can be profusely found in the literature.³⁷ Fig S11 in the ESI[†] illustrates the results of the GC-FID monitoring profile of the oxidation of MF by H₂O₂ in the presence of **1**, after 60, 120 and 180 min of reaction. Two substrates are fully converted into the corresponding oxidized products and, in accordance with the above-mentioned results. The catalyst **1** seems to be more efficient for DBT oxidation. In fact, after 50 min of reaction, DBT is hardly observed in the corresponding chromatogram, whereas the BT is still present.

Conclusions

In conclusion, catalyst **1** was synthesized by a simple and controllable one-pot reaction system, and applied to the oxidation of recalcitrant sulfur compounds. An efficient and environmental friendly oxidation experiment for BT and DBT in CH₃CN catalytic system at room temperature is demonstrated. Excellent organosulfur compound conversion values were obtained even in high ratio of substrate to catalyst (up to 1500), but the recyclability was found to be insufficient under the mild reaction conditions. The high potential of **1** for application in ODS processes was verified through the results achieved in the oxidation of model fuels by H₂O₂. These results indicate that **1** is a promising heterogeneous catalyst for ODS. In the near future, we intend to develop our studies by using stable POM-based heterogeneous catalysts in the oxidation of this kind of recalcitrant compounds, and also in real fuel samples.

Acknowledgements

We gratefully acknowledge financial support from the National Natural Science Foundation of China and Natural Science Foundation of Henan Province.

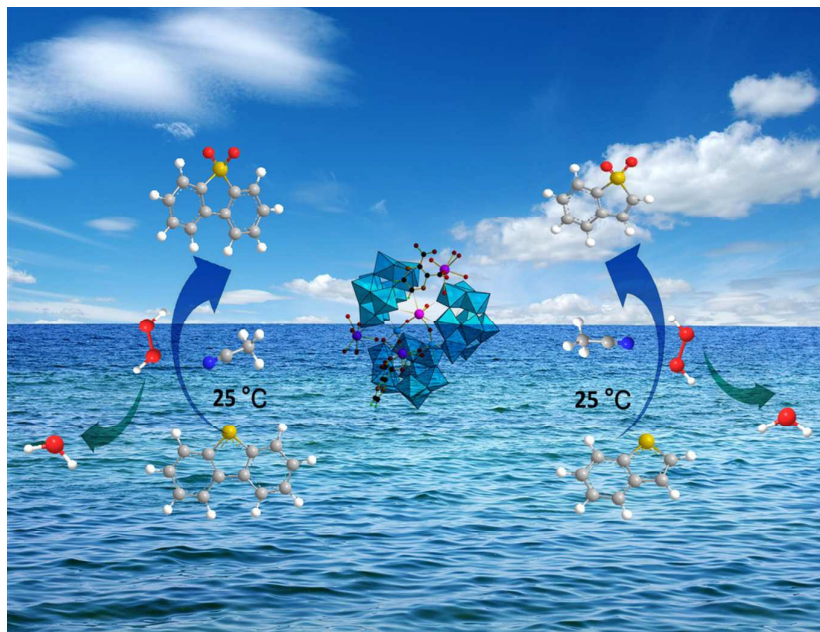
Notes and references

- (a) C. L. Hill, *Chem. Rev.*, 1998, **98**, 1–2; (b) D.-L. Long, E. Burkholder and L. Cronin, *Chem Soc Rev*, 2007, **36**, 105–121; (c) A. Proust, R. Thouvenot and P. Gouzerh, *Chem. Commun.*, 2008, **16**, 1837–1852; (d) U. Kortz, A. Müller, J. van Slageren, J. Schnack, N. S. Dalal and M. Dressel, *Coord. Chem. Rev.*, 2009, **253**, 2315–2327.
- (a) I. V. Kozhevnikov, *Chem. Rev.*, 1998, **98**, 171–198; (b) D. E. Katsoulis, *Chem. Rev.*, 1998, **98**, 359–387; (c) W. Zhu, W. Huang, H. Li, M. Zhang, W. Jiang, G. Chen and C. Han, *Fuel Process. Technol.*, 2011, **92**, 1842–1848.
- (a) S.-T. Zheng and G.-Y. Yang, *Chem. Soc. Rev.*, 2012, **41**, 7623–7646; (b) H. N. Miras, J. Yan, D.-L. Long and L. Cronin, *Chem. Soc. Rev.*, 2012, **41**, 7403–7430; (c) S.-S. Wang and G.-Y. Yang, *Chem. Rev.*, 2015, **115**, 4893–4962. (d) K. Wassermann, M. H. Dickman and M. T. Pope, *Angew. Chem., Int. Ed. Engl.*, 1997, **36**, 1445–1448; (e) F. Hussain, B. Spingler, F. Conrad, M. Speldrich, P. Kögerler, C. Boskovic and G. R. Patzke, *Dalton Trans.*, 2009, **23**, 4423–4425.
- (a) C.-D. Wu, C.-Z. Lu, H.-H. Zhuang and J.-S. Huang, *J. Am. Chem. Soc.*, 2002, **124**, 3836–3837; (b) J.-Y. Niu, M.-L. Wei, J.-P. Wang and D.-B. Dang, *Eur. J. Inorg. Chem.*, 2004, **1**, 160–170; (c) H.-Y. An, Y.-G. Li, D.-R. Xiao, E.-B. Wang and C.-Y. Sun, *Cryst. Growth Des.*, 2006, **6**, 1107–1112.
- (a) R. D. Peacock and T. J. R. Weakley, *J. Chem. Soc. A.*, 1971, 1836–1839; (b) M. Sadakane, A. Ostuni and M. T. Pope, *J. Chem. Soc. Dalton Trans.*, 2002, **1**, 63–67; (c) M. Sadakane, M. H. Dickman and M. T. Pope, *Inorg. Chem.*, 2001, **40**, 2715–2719; (d) J. Cao, S. Liu, R. Cao, L. Xie, Y. Ren, C. Gao and L. Xu, *Dalton Trans.*, 2008, 115–120; (e) C. Boglio, G. Lenoble, C. Duhayon, B. Hasenknopf, R. Thouvenot, C. Zhang, R. C. Howell, B. P. Burton-Pye, L. C. Francesconi, E. Lacôte, S. Thorimbert, M. Malacria, C. Afonso and J.-C. Tabet, *Inorg. Chem.*, 2006, **45**, 1389–1398; (f) W.-D. Wang, X.-X. Li, W.-H. Fang and G.-Y. Yang, *J. Clust. Sci.*, 2011, **22**, 87–95; (g) B. S. Bassil, M. H. Dickman, B. von der Kammer and U. Kortz, *Inorg. Chem.*, 2007, **46**, 2452–2458.
- J. Zhao, Q. Han, D. Shi, L. Chen, P. Ma, J. Wang and J. Niu, *J. Solid State Chem.*, 2011, **184**, 2756–2761.
- K. Wassermann, M. H. Dickman and M. T. Pope*, *Angew. Chem.* 1997, **109**, 1513–1516.
- F. Hussain and G. R. Patzke, *CrystEngComm*, 2011, **13**, 530–536.
- K. Wassermann and M. T. Pope, *Inorg. Chem.*, 2001, **40**, 2763–2768.
- F. Hussain, F. Conrad and G. Patzke, *Angew. Chem. Int. Ed.*, 2009, **48**, 9088–9091.
- F. Hussain, R. W. Gable, M. Speldrich, P. Kögerler and C. Boskovic, *Chem Commun*, 2009, **3**, 328–330.
- W. L. Chen, Y. G. Li, Y. H. Wang, E. B. Wang and Z. M. Su, *Dalton Trans.*, 2007, **38**, 4293–4301.
- C. Ritchie, M. Speldrich, R. W. Gable, L. Sorace, P. Kögerler and C. Boskovic, *Inorg. Chem.*, 2011, **50**, 7004–7014.
- C. Ritchie, E. G. Moore, M. Speldrich, P. Kögerler and C. Boskovic, *Angew. Chem. Int. Ed.*, 2010, **49**, 7702–7705.
- S. Li, Y. Wang, P. Ma, J. Wang and J. Niu, *CrystEngComm*, 2014, **16**, 10746–10749.
- Y. Wang, X. Sun, S. Li, P. Ma, J. Wang and J. Niu, *Dalton Trans.*, 2015, **44**, 733–738.
- Y. Wang, X. Sun, S. Li, P. Ma, J. Niu and J. Wang, *Cryst. Growth Des.*, 2015, **15**, 2057–2063.
- A. M. Kirillov and G. B. Shul'pin, *Coord. Chem. Rev.*, 2013, **257**, 732–754.
- (a) R.J. Butcher, J.W. Overman and E. Sinn, *J. Am. Chem. Soc.*, 1980, **102**, 3276–3278; (b) C.J. O'Connor, C.L. Klein, R.J. Majeste and L.M. Trefonas, *Inorg. Chem.*, 1982, **21**, 64–67.
- T. Ueda, K. Yamashita and A. Onda, *Appl. Catal. Gen.*, 2014, **485**, 181–187.

ARTICLE

Journal Name

- 21 (a) M. C. Carreño, *Chem. Rev.*, 1995, **95**, 1717–1760; (b) E. N. Prilezhaeva, *Russ. Chem. Rev.*, 2000, **69**, 367–408; (c) A.-N. R. Alba, X. Companyó and R. Rios, *Chem. Soc. Rev.*, 2010, **39**, 2018–2033; (d) R. Bentley, *Chem. Soc. Rev.*, 2005, **34**, 609; (e) R. Villar, I. Encio, M. Migliaccio, M. J. Gil and V. Martínez-Merino, *Bioorg. Med. Chem.*, 2004, **12**, 963–968.
- 22 (a) V. Chandra Srivastava, *RSC Adv*, 2012, **2**, 759–783; (b) K.-E. Jeong, T.-W. Kim, J.-W. Kim, H.-J. Chae, C.-U. Kim, Y.-K. Park and S.-Y. Jeong, *Korean J. Chem. Eng.*, 2013, **30**, 509–517; (c) H. Li, W. Zhu, Y. Wang, J. Zhang, J. Lu and Y. Yan, *Green Chem.*, 2009, **11**, 810–815; (d) H. Mirhoseini and M. Taghdiri, *Fuel*, 2016, **167**, 60–67; (e) Z. Jiang, H. Lü, Y. Zhang and C. Li, *Chin. J. Catal.*, 2011, **32**, 707–715.
- 23 (a) P. S. Kulkarni and C. A. M. Afonso, *Green Chem.*, 2010, **12**, 1139; (b) C. Yansheng, L. Changping, J. Qingzhu, L. Qingshan, Y. Peifang, L. Xiumei and U. Welz-Biermann, *Green Chem.*, 2011, **13**, 1224. (c) H. Lü, W. Ren, H. Wang, Y. Wang, W. Chen and Z. Suo, *Appl. Catal. Gen.*, 2013, **453**, 376–382; (d) M. Zhang, W. Zhu, S. Xun, H. Li, Q. Gu, Z. Zhao and Q. Wang, *Chem. Eng. J.*, 2013, **220**, 328–336.
- 24 U. Kortz, M. G. Savelieff, B. S. Bassil and M. H. Dickman, *Angew. Chem., Int. Ed.*, 2001, **40**, 3384–3386.
- 25 (a) G. M. Sheldrick, *SHELXS97, Program for Crystal Structure Solution*, University of Göttingen, Göttingen, Germany, 1997; (b) R. Dessapt, D. Kervern, M. Bujoli-Doeuff, P. Deniard, M. Evain and S. Jobic, *Inorg. Chem.*, 2010, **49**, 11309–11316.
- 26 S. M. G. Pires, M. M. Q. Simões, I. C. M. S. Santos, S. L. H. Rebelo, F. A. A. Paz, M. G. P. M. S. Neves and J. A. S. Cavaleiro, *Appl. Catal. B Environ.*, 2014, **160–161**, 80–88.
- 27 H. H. Thorp, *Inorg. Chem.*, 1992, **31**, 1585–1588.
- 28 J. Niu, K. Wang, H. Chen, J. Zhao, P. Ma, J. Wang, M. Li, Y. Bai and D. Dang, *Cryst. Growth Des.*, 2009, **9**, 4362–4372.
- 29 (a) P. Mahata, K. V. Ramya and S. Natarajan, *Chem. - Eur. J.*, 2008, **14**, 5839–5850; (b) B. D. Chandler, D. T. Cramb and G. K. H. Shimizu, *J. Am. Chem. Soc.*, 2006, **128**, 10403–10412.
- 30 (a) X. Zhang, Y. Shi and G. Liu, *Catal. Sci. Technol.*, 2016, **6**, 1016–1024; (b) J. Zhang, A. Wang, X. Li and X. Ma, *J. Catal.*, 2011, **279**, 269–275.
- 31 E. Rafiee and N. Nobakht, *J. Mol. Catal. Chem.*, 2015, **398**, 17–25.
- 32 (a) G. Luo, L. Kang, M. Zhu and B. Dai, *Fuel Process. Technol.*, 2014, **118**, 20–27; (b) L. Tang, G. Luo, M. Zhu, L. Kang and B. Dai, *J. Ind. Eng. Chem.*, 2013, **19**, 620–626.
- 33 S. Ribeiro, A. D. S. Barbosa, A. C. Gomes, M. Pillinger, I. S. Gonçalves, L. Cunha-Silva and S. S. Balula, *Fuel Process. Technol.*, 2013, **116**, 350–357.
- 34 X. Hu, Y. Lu, F. Dai, C. Liu and Y. Liu, *Microporous Mesoporous Mater.*, 2013, **170**, 36–44.
- 35 (a) C. Yang, Q. Jin, H. Zhang, J. Liao, J. Zhu, B. Yu and J. Deng, *Green Chem.*, 2009, **11**, 1401–1405; (b) X. Zhang, Y. Shi and G. Liu, *Catal. Sci. Technol.*, 2016, **6**, 1016–1024.
- 36 (a) S. Ribeiro, C. M. Granadeiro, P. Silva, F. A. Almeida Paz, F. F. de Biani, L. Cunha-Silva and S. S. Balula, *Catal. Sci. Technol.*, 2013, **3**, 2404–2414; (b) J. Xu, S. Zhao, W. Chen, M. Wang and Y.-F. Song, *Chem. - Eur. J.*, 2012, **18**, 4775–4781; (c) A. Nisar, Y. Lu, J. Zhuang and X. Wang, *Angew. Chem.*, 2011, **123**, 3245–3250; (d) H. Li, X. Jiang, W. Zhu, J. Lu, H. Shu and Y. Yan, *Ind. Eng. Chem. Res.*, 2009, **48**, 9034–9039; (e) B. Zhu, L.-K. Yan, W. Guan and Z.-M. Su, *Dalton Trans.*, 2015, **44**, 9063–9070.
- 37 (a) X.-M. Yan, P. Mei, L. Xiong, L. Gao, Q. Yang and L. Gong, *Catal. Sci. Technol.*, 2013, **3**, 1985–1992; (b) L. S. Nogueira, S. Ribeiro, C. M. Granadeiro, E. Pereira, G. Feio, L. Cunha-Silva and S. S. Balula, *Dalton Trans*, 2014, **43**, 9518–9528; (c) C. M. Granadeiro, S. O. Ribeiro, M. Karmaoui, R. Valença, J. C. Ribeiro, B. de Castro, L. Cunha-Silva and S. S. Balula, *Chem. Commun.*, 2015, **51**, 13818–13821.



A new polytungstoarsenate:

$\text{K}_6\text{LiH}_6[\text{Ce}_4(\text{H}_2\text{O})_{14}(\text{pzdc})(\text{H}_2\text{pzdc})\text{As}_3\text{W}_{29}\text{O}_{103}]\cdot 22\text{H}_2\text{O}$ (**1**) (H_2pzdc = 2,3-pyrazinedicarboxylic acid) is synthesized through conventional aqueous solution by introducing organic ligand pyrazine dicarboxylate acid into the arsenotungstates system. The catalytic activity of compound **1** was evaluated in the oxidation of two organosulfur compounds (BT and DBT) by H_2O_2 in acetonitrile at room temperature. Two substrates were oxidized to their corresponding sulfones with high conversion and selectivity. Considering the remarkable results achieved, the **1**/ H_2O_2 / CH_3CN system was studied in the oxidation of model fuels (MF) including a mixture of BT and DBT in octane. As a result, the organosulfur compounds in the model fuels were fully converted into their corresponding sulfones.